J. Physiol. (1978), **277**, *pp.* 483–506
With 11 *text-figures*
Printed in Great Britain

CONTRACTILE ACTIVATION BY VOLTAGE CLAMP DEPOLARIZATION OF CUT SKELETAL MUSCLE FIBRES

BY L. KOVÁCS* AND M. F. SCHNEIDER

From the Department of Physiology, University of Rochester, School of Medicine and Dentistry, Rochester, New York 14642, U.S.A.

(*Received 17 March 1977*)

SUMMARY

1. Single frog skeletal muscle fibres bathed in a relaxing solution were cut close to the tendon and mounted across a single Vaseline gap so that a short segment of intact terminated fibre extended beyond one side of the gap.

2. A compensating circuit, set with a micro-electrode in the terminated fibre segment, was used both to correct total current for external current crossing the gap and to correct pool voltage for the voltage drop across the fibre segment in the gap.

3. The micro-electrode was then removed and the fibre voltage-clamped using the compensating circuit. This allowed movement without damage under controlled voltage.

4. Strength–duration curves for contraction thresholds of cut fibres exposed externally to TTX Ringer solution and internally to a predominantly K glutamate solution were similar to strength–duration curves reported for intact fibres.

5. The change from TTX Ringer to a predominantly $(TEA)_2SO_4$ external solution shifted the strength–duration curve for cut fibre contraction thresholds in the negative direction as reported for intact fibres.

6. When studied at 3–4 °C, fibres from warm-adapted frogs appeared to have higher contraction thresholds than fibres from cold-adapted frogs.

7. Delayed rectifier currents recorded from cut fibres were similar to those reported for intact fibres.

INTRODUCTION

It is well established that contraction of skeletal muscle fibres is initiated by fibre depolarization (Kuffler, 1946; Sten-Knudsen, 1954, 1960; Hodgkin & Horowicz, 1960) and that to be effective, the depolarization must include membranes of the transverse (T–) tubular system (Huxley & Taylor, 1958; Huxley & Straub, 1958). It is also well established that the myofilaments in skeletal muscle are converted from an inhibited to a disinhibited mechanochemical state by calcium binding to troponin molecules on the thin filaments (cf. Ebashi, Endo & Ohtsuki, 1969). Direct evidence for an increase in myoplasmic calcium following an action potential has been presented (Jöbsis & O'Connor, 1966; Taylor, Rüdel & Blinks, 1975) and it is

* Present address: Department of Physiology, Medical University of Debrecen, H-4012 Debrecen, Hungary.

generally accepted that both the source of and the eventual sink for this calcium is the sarcoplasmic reticulum (Ebashi & Endo, 1968). The way in which T-tubule depolarization gives rise to calcium release in the sarcoplasmic reticulum is, however, not well understood.

In the past, two general types of muscle fibre preparation have been used in studies of excitation–contraction coupling. The first is the intact fibre, in which contraction is initiated by the normal physiological stimulus of T-tubule depolarization. The second is the skinned (Natori, 1954) or split (Nakajima & Endo, 1973) muscle fibre. Skinned or split fibres have the advantage that the medium bathing the sarcoplasmic reticulum and contractile filaments is directly accessible for experimental manipulation. However, since they lack the membrane barrier between fibre interior and exterior which is present in intact fibres, the possibility of initiating calcium release by controlled T-tubule depolarization is made difficult or impossible. Instead, calcium release in skinned or split fibres is generally initiated by various types of solution change which are thought to act directly on the sarcoplasmic reticulum (Costantin & Podolsky, 1967; Endo, Tanaka & Ogawa, 1970; Ford & Podolsky, 1972; Nakajima & Endo, 1973). In the present report we consider a new preparation for studying *E–C* coupling, the cut muscle fibre. Cut fibres combine accessibility of the internal medium with the ability to initiate contraction by fibre depolarization.

Cut skeletal muscle fibres were recently introduced by Hille & Campbell (1976) and found to be suitable for studying muscle fibre sodium currents under voltage-clamp conditions. However, the procedure used by Hille & Campbell resulted in fibres which were mechanically inactive. We have modified the procedure so as to produce cut fibres which contracted on depolarization. Such fibres also exhibited normal delayed rectifier currents, which were not present in the fibres examined by Hille & Campbell (1976).

This report presents the methods we have developed to prepare and study mechanical and electrical activity of cut fibres. It also presents evidence supporting the conclusions that contractile activation and delayed rectification in cut fibres are relatively little effected by the preparative procedure. A report of optical studies in which cut fibres were used for investigating intermediate steps in *E–C* coupling has already appeared (Kovács & Schneider, 1977*a*) and further studies using cut fibres are in progress. An abstract of parts of this work has previously been presented (Kovács & Schneider, 1977*b*).

METHODS

Fibre preparation and mounting

Frog (*Rana pipiens*) semitendinosus or ileofibularis muscles were isolated and dissected down to thin layers of fibres, fibre bundles or single fibres at room temperature in Ringer's solution (115 mM-NaCl, 2·5 mM-KCl, 1·8 mM-$CaCl_2$, 1 mM-Tris – maleate buffer). The solution bathing the preparation was then changed to a high potassium, calcium-free 'relaxing' solution (120 mM-potassium glutamate, 2 mM-magnesium chloride, 0·01 mM-EGTA, 5 mM-Tris-maleate buffer), also at room temperature. Following relaxation from the resulting potassium contracture, a single fibre was isolated for a distance of about 0·5–1 cm from its tendon and cut. In order to avoid slow fibres, the tonic bundle of the ileofibularis was not used.

The cut fibre was transferred to a lucite experimental chamber containing two pools separated by a wall about 550 μm wide. A small groove in the top surface of the wall ran from one pool to the other. For fibre mounting the groove was partially filled with Vaseline and the

chamber was filled with excess relaxing solution so that the wall separating the pools was covered by solution. The fibre was mounted so as to run from one pool to the other via the groove as shown in Fig. 1. The tendon was clamped to a movable block in the closed end pool (pool C) and the cut end was clamped to a similar movable block in the open end pool (pool A). By positioning the blocks the length l_c of the intact terminated fibre segment in pool C was set at about 500 μm and its sarcomere length S was set at about 2·5–3·0 μm. To minimize the diffusion distance and impedance of the cut fibre segment in pool A, the fibre was notched with fine scissors a few tenths of a mm from the wall in pool A.

The space around the fibre in the groove was filled with Vaseline and the upper surface of the wall between pools was covered with Vaseline. A leucite partition was placed on the wall so that its edge was even with the pool C side of the wall. As shown diagrammatically in Fig. 1,

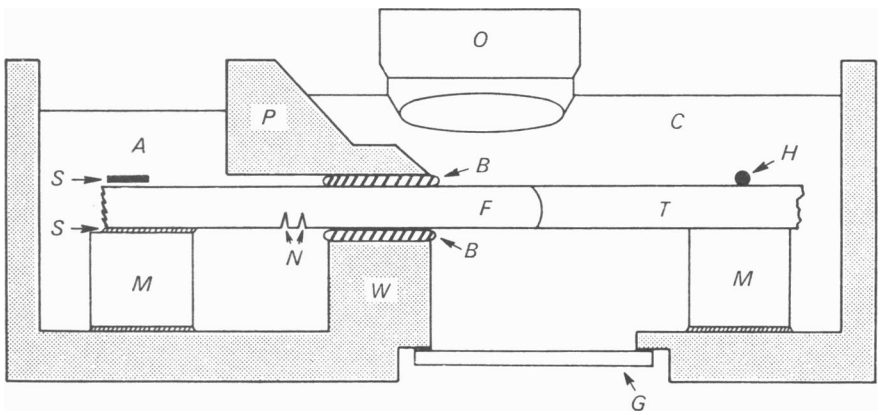

Fig. 1. Diagrammatic representation of a cut fibre mounted in the experimental chamber. A vertical section through the middle of the chamber is illustrated. F, muscle fibre; T, tendon; A, open end pool; C, closed end pool; W, wall separating the pools, with groove for accommodating the fibre; B, Vaseline seals between fibre and groove and between wall and partition; N, notches cut in fibre; M, movable blocks; H, wire clamp for holding the tendon to the block in pool C; S, Vaseline and a piece of Scotch tape for holding cut end of fibre to block in pool A; P, partition placed above the wall; G, glass coverslip used as chamber floor below fibre in pool C; O, water immersion objective.

the partition was shaped so as to extend pool C toward pool A above the wall. This was necessary to accommodate the water immersion objective used to observe the intact fibre segment. After positioning the partition the solution level was lowered so as to produce two pools separated by the fibre segment in the Vaseline gap (Fig. 1). The pool A solution was changed to relaxing solution to which 0·5 mM-ATP and 1 mM-EGTA were added (solution A).

Pool current and voltage measurements

The electrical connexions to the chamber are shown schematically in Fig. 2. The voltage difference V_P between the two pools (A minus C) was recorded using two agar bridges and unity-gain voltage followers, followed by a differential amplifier (amplifiers A4–6, Fig. 2). Pool C was held at virtual ground using two other agar bridges and a current-measuring operational amplifier circuit (amplifiers A7–9, Fig. 2). The total current I applied to the fibre, monitored as the voltage drop across the resistor R_I in the feed-back loop of amplifier A7, was given by V_I/R_I. Pool A was connected either to a voltage source E_P or to the output of a voltage clamp amplifier (A10) via a fifth agar bridge and a switch. All bridges contained 2% agar in 3 M potassium chloride and contacted 3 M potassium chloride pools fitted with silver/silver chloride pellet electrodes.

Preliminary electrical check of fibre and gap

For initial electrical checks pool A was connected to E_P which applied 15 or 20 mV pulses from a steady level of 0 mV. The resulting steady change in V_I was generally less than 1·5 or 2·0 mV, indicating a net effective resistance (fibre in parallel with external leak) of more than 1 MΩ. If the Vaseline seal were poorly made or if the fibre were damaged, much higher currents were observed and the fibre was discarded.

When a fibre with suitable resistance between pools was obtained, pool C was changed to either Ringer solution or to solution C (75 mM-$(TEA)_2SO_4$, 5 mM-Rb_2SO_4, 7·5 mM-total Ca SO_4, 5 mM-Tris – maleate buffer) and the chamber cooled using a Peltier device (Cambion). The temperature, monitored using a thermistor positioned near the fibre in pool C, was 2–4 °C. Both external solutions contained 10^{-7} g/ml. (TTX) tetrodotoxin and all solution pH levels were set at 7·0 ± 0·1 at room temperature.

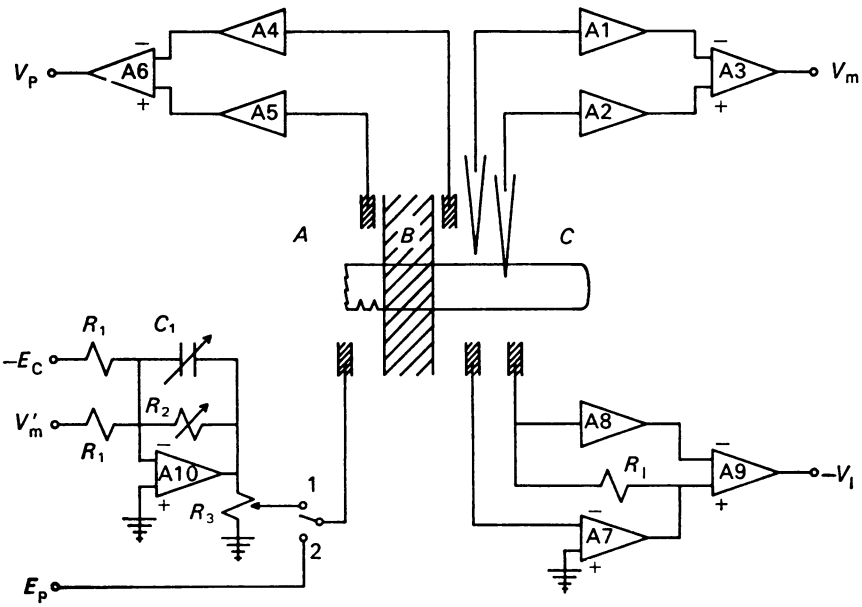

Fig. 2. Voltage and current recording circuits and voltage control circuit used with cut fibres. A1 and A2 were unity gain FET input voltage followers having driven shields (input capacitance 1–2 pF). A3 represents one channel of a Tektronix 3A3 amplifier in a Tektronix 565 oscilloscope. A4 through A9 were made using Signetics 536 operational amplifiers connected in standard feed-back configurations. A4, A5 and A8 were high input impedance unity gain voltage followers. A6 and A9 were unity gain differential amplifiers having respective time constants of 10^{-7} sec and 10^{-5} sec. A7 was connected as a current measuring amplifier (R_I = 100 kΩ) using two agar bridges so as to hold pool C at virtual ground. Switch position 2 was used for applying voltage E_P directly to pool A whereas position 1 was used for voltage clamping. The control amplifier A10 was Teledyne-Philbrick 1434 with R_1 = 10 kΩ, 10 kΩ ≤ R_2 ≤ 10 MΩ, R_3 = 1·1 kΩ and 30 ≤ C_1 ≤ 3000 pF.

The fibre was observed using a compound microscope (American Optical Microstar) equipped with a 40 × 0·75 N.A. water-immersion objective (Zeiss) and 10 × widefield eyepieces (Nikon). In the first experiments sarcomere lengths were determined by counting the number of sarcomeres in 30 μm using an eyepiece scale. In later experiments the length of ten sarcomeres was measured using a filar micrometer eyepiece (American Optical 426).

Direct and indirect monitoring of fibre membrane potentials

Direct measurements of the membrane potential V_m of the closed fibre segment in pool C were made using internal and external micro-electrodes connected to unity-gain FET input amplifiers followed by a differential amplifier (amplifiers A1–3 in Fig. 2). Micro-electrodes were filled with 3 M-potassium chloride and had resistance of 15–30 MΩ. In order to measure V_m at the start or input of the closed segment, the internal electrode was inserted into the segment in pool C as close as possible to the gap (generally within 50 μm) using a fine horizontal translation stage (Lansing) which supported a coarse micromanipulator.

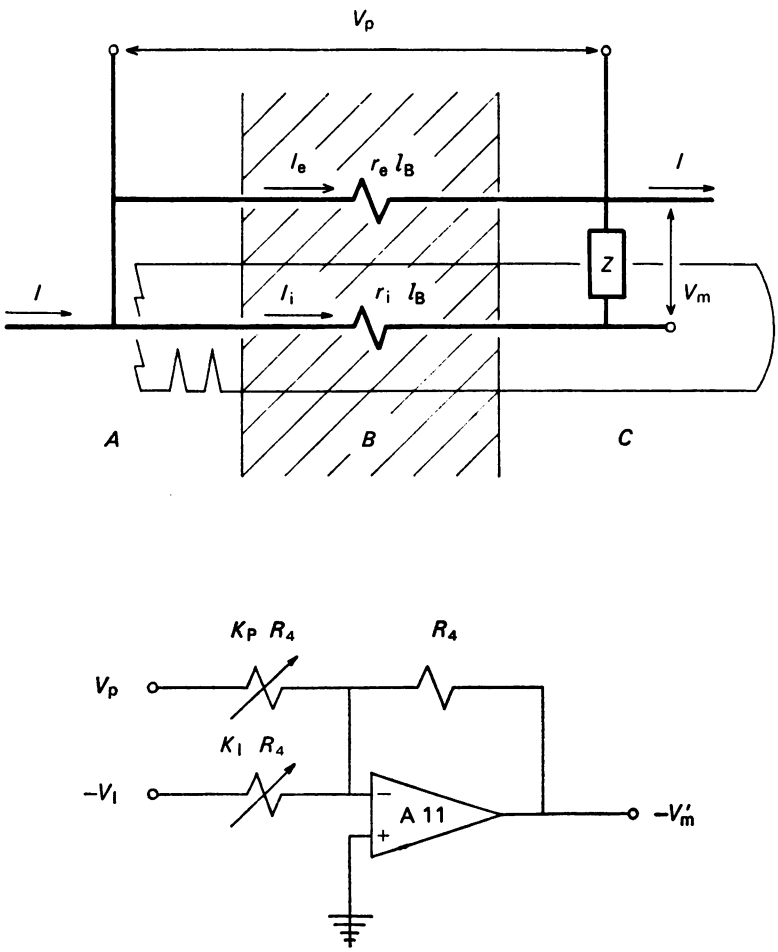

Fig. 3. Equivalent circuit for a cut fibre and the operational amplifier circuit used for monitoring fibre membrane potential using external recording. Upper: A, B and C as in Fig. 1. Z represents the input impedance of the terminated intact fibre segment in pool C. $r_i l_B$ and $r_e l_B$ represent the internal and external longitudinal resistances across the Vaseline gap (B) of length l_B. The impedance of the cut segment in pool A is considered negligible. The total current I applied to the fibre crosses the gap as internal I_i and external I_e current components. V_P, V_m and a voltage V_I proportional to I are recorded using the circuit in Fig. 2. Lower: amplifier A11 was Signetics 536 with $0 \leqslant K_P \leqslant 5$, $0 \leqslant K_I \leqslant 2$ and $R_4 = 10$ kΩ. The method of adjusting K_P and K_I so that $V'_m = V_m$ is described in the text.

Fibre membrane potentials were indirectly monitored with an operational amplifier compensating circuit (Fig. 3*B*) which used V_P and V_I to electronically generate a potential V'_m equal to the fibre membrane potential just beyond the gap in pool *C*. When properly adjusted, the compensating circuit generated V'_m by correcting V_P for the voltage drop across the series resistance arising from the myoplasm of the length of fibre in the gap. This correction was similar to that carried out in standard 'compensated feed-back' (Hodgkin, Huxley & Katz, 1952) used in squid axon voltage clamping. To perform the series resistance compensation, the circuit also had to correct the total recorded current for leakage current between pools outside the fibre. As described in the Theory section, adjustment of the compensating circuit required comparison of V'_m with the V_m directly measured using a micro-electrode inserted in the fibre just beyond the gap in pool *C*. However, once the compensating circuit was properly adjusted, the micro-electrode could be removed and V'_m used to monitor membrane potential. It was then possible to apply depolarizing pulses beyond contraction threshold without fibre damage while still monitoring the indirectly recorded membrane potential.

Voltage-clamping

After properly adjusting the compensating circuit, a voltage clamp circuit (amplifier A10 and feed-back circuit, Fig. 2) was used to hold V'_m close to the command voltage level E_C. The clamp gains used in these experiments were about 80 ×, produced by about 100 × gain on amplifier A10 together with a factor of about 0·8 of R_3 (Fig. 2). Since V'_m was the controlled voltage, misadjustment of the compensating circuit would tend to make the clamp unstable. In practice, the compensating circuit was generally found to be out of adjustment on checking with a micro-electrode when V'_m oscillations and notchy current records were seen. With proper compensating circuit adjustment, clamp feed-back capacitance was set to give a rapidly rising V'_m with only small overshoot.

Contraction threshold

Strength-duration curves for the contraction threshold were determined by applying a sequence of depolarizing pulses of constant duration but increasing amplitude. The amplitude was increased until a movement was seen by the observer using the microscope at 400 ×. A 1 or 2 mV increase in amplitude was generally sufficient to go from no observed movement to definite movement. The sequence was initially carried out using the longest pulse duration, was repeated with successively shorter pulse durations down to 5 msec and was finally repeated using the longest duration. V'_m was not recorded during the process of determining the strength–duration curve. The pulse amplitude was taken as the pulse command voltage multiplied by the ratio of − 100 mV divided by the steady command voltage required to hold the fibre at − 100 mV. For subsequent pulses in the same range the steady level of V'_m was within 1 mV of the value calculated using the command pulse. The pulse duration was taken as the command pulse duration. With non-square pulses such measures of amplitude and duration introduce inaccuracies, with greatest relative error being applicable to the shortest pulses. To minimize this problem, pulses shorter than 5 msec were not employed.

Electrical measurements

During initial adjustment of the compensating circuit, E_P pulses of 15–20 mV were applied to pool *A* from a base line E_P level of 0 mV. The resulting steady displacements of V_P, V_I and V_m during the pulse were read directly from the oscilloscope and recorded for use in rough calculations of fibre electrical properties. Under voltage clamp conditions, more precise electrical measurements were made by recording signals for later analysis. Two different methods were employed. In some cases oscilloscope records were photographed and voltages subsequent determined from measurements of projected images. In other cases signals were digitized, sent to a small laboratory computer (Digital Equipment Corp., PDP 8-E), stored on magnetic tape and subsequently analysed using appropriate computer programs. The data sent to the computer consisted of a sequence of integrals of each of two signals carried out over successive 1 msec intervals using two voltage-to-frequency converters (Anadex 1700-5044) and a digital counting circuit clocked in precise synchrony with a digital pulse timing unit (W-P Instruments, Series 830). As previously described (Schneider & Chandler, 1976; Chandler, Rakowski & Schneider, 1976*a*) this method of digitization is convenient for evaluating both the charge carried by capacitative transients and steady levels of voltages of interest.

THEORY

Voltage recording using the single gap

According to the circuit in Fig. 3*A* the voltage V_m at the input of the closed fibre segment is given by the pool voltage minus the voltage drop across the internal resistance of the length l_B of fibre in the gap. Thus,

$$V_m = V_P - r_i l_B I_i, \tag{1}$$

where I_i is the internal current and r_i is the fibre internal resistance per unit length. I_i is equal to the total current I between the pools, measured as V_I/R_I (Fig. 2), minus the external current I_e traversing the leak resistance $r_e l_B$ connecting the pools so that

$$I_i = \frac{V_I}{R_I} - \frac{V_P}{r_e l_B}, \tag{2}$$

where r_e is the external resistance per unit length in the gap. Substituting (2) into (1) and rearranging gives

$$V_m = V_P\left(\frac{r_i + r_e}{r_e}\right) - \frac{V_I r_i l_B}{R_I}. \tag{3}$$

It follows from eqn. (3) that it should be possible to monitor V_m using V_P and V_I. This was accomplished using an operational amplifier compensating circuit (Fig. 3*B*) which has an output voltage V_m' given by

$$V_m' = \frac{V_P}{K_P} - \frac{V_I}{K_I}. \tag{4}$$

The values of the scale factors K_P and K_I were determined by the settings of two ten-turn potentiometers in the compensating circuit. When the compensating circuit was properly adjusted, K_P and K_I were set equal to $r_e/(r_i + r_e)$ and $R_I/r_i l_B$ so that $V_m' = V_m$.

The preceding analysis and the simplified equivalent circuit in Fig. 3*A* have assumed the fibre membrane conductance within the gap to be negligible. A more general analysis presented in the Appendix demonstrates, however, that eqn. (3) and the compensation procedure are valid for both steady-state and transient situations, independent of the membrane conductance in the gap.

Adjusting the compensating circuit

In order to adjust the compensating circuit a square voltage pulse was applied to the open end pool via E_P (Fig. 2). This caused the same pulse in V_P (Fig. 4*C*) since the closed end pool was held at virtual ground. A micro-electrode was inserted in the closed fibre segment close to the gap so that V_m provided a direct measure of the closed segment input voltage (Fig. 4*B*). At the ON of the V_P pulse there was no instantaneous change in V_m. At this instant $V_P - r_i l_B I_i = 0$ (eqn. (1)). Then, as the capacitance of the closed segment became charged, V_m rose to its steady level following a time course governed by the decline of I_i. The events at pulse OFF were similar.

Since V_P/K_P was a square pulse having no transient component, the size of the transient component of V_m' depended on the value of K_I and was independent of

the value of K_P (eqn. (4)). Under this condition adjusting the values of K_I and K_P so that $V'_m = V_m$ was relatively straightforward. The first step was to set K_I so that the transient phase of V'_m exactly matched the rise or fall of V_m. Then K_P was set so as to eliminate the jump in V'_m at pulse ON and OFF. At these settings $V'_m = V_m$ (Fig. 4*b*, *e*).

The value thus selected for K_I scaled the component of V_I due to I_i so that the same voltage was subtracted from V_P in V'_m (eqn. (4)) as I_i produced across $r_i l_B$ (eqn. (1)). The component of V_I due to I_e was necessarily also scaled by the same factor and subtracted. But since I_e is proportional to V_P, the effect of I_e was eliminated by selecting a value of K_P which scaled V_P so as to just balance the I_e component of V_I/K_I.

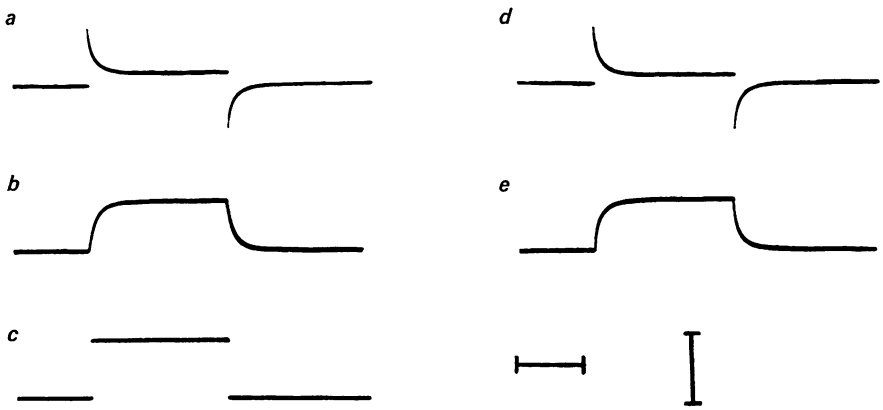

Fig. 4. Signals recorded in response to a V_P pulse after having set the compensating circuit. The voltages represented by each trace are (*a*) V_I, (*b*) V_m, (*c*) V_P, (*d*) V'_I and (*e*) V'_m. Horizontal calibration is 20 msec. Vertical calibration for *a* is 10 mV, which corresponds to 100 nA, and 40 mV for *b* to *e*. The compensating circuit had $K_P = 0{\cdot}922$ and $K_I = 0{\cdot}234$ so that the 40 mV V'_I calibration in *d* corresponds to 94 nA. Pools *A* and *C* contained solutions *A* and *C*. Fibre 73 with $l_c = 355\ \mu m$, $d = 64\ \mu m$ and *S* not measured (3·3 °C).

Use of a V_P pulse was convenient for adjusting the compensating circuit since in that case I_i but not I_e had a transient component. However, the description in the preceding paragraph and the analysis in eqns. (1)–(4) apply to all V_P time courses. Thus, although for convenience the compensation was adjusted using a V_P pulse, it was proper for any V_P wave form (Fig. 5*A*).

After adjusting K_I and K_P, the micro-electrode could be removed from the fibre. As long as $r_i l_B$ and $r_e l_B$ remained constant, V'_m could be used to monitor the input voltage of the closed fibre segment. It should be stressed that since the input impedance Z_{IN} of the closed fibre segment does not appear in eqn. (3), the proper values of K_P and K_I were independent of Z_{IN}. Thus V'_m would equal V_m even though Z_{IN} changed considerably, provided only that the scale factors K_P and K_I had been properly adjusted.

Measuring fibre input current using the single gap

Since one function of the compensating circuit was to correct V_I for I_e, adjustment of K_I and K_P allowed I_i to be monitored independently of I_e. With the compensating circuit properly adjusted, $V'_m = V_m$ and eqn. (1) can be rewritten as

$$r_i l_B I_i = V_P - V'_m. \quad (5)$$

The signal $V_P - V'_m$, which will be referred to as V'_I was thus proportional to I_i. Under proper compensation $r_i l_B = R_I/K_I$ so that

$$I_i = V'_I(K_I/R_I). \quad (6)$$

The value of K_I was determined directly from the setting of the ten turn calibrated variable resistor in the compensating circuit so that the scale factor for relating V'_I to I_i was known.

Despite the unrestricted validity of eqn. (3) which relates V_m to V_P using total current, equations such as (1), (2), (5) and (6) which explicitly involve internal or external current are strictly valid only for the case of negligible membrane conductance in the gap. The fractional error introduced by using $V'_I K_I/R_I$ as a measure of the steady current entering the terminated segment is analysed and evaluated in the Appendix for $V'_m = V_m$. Keeping other parameters constant, the fractional error decreases with either increasing membrane resistance in the gap, decreasing l_B, increasing r_e or decreasing R_{IN}. For a typical fibre studied using solution *C* in pool *C*, the steady current measured using the compensating circuit would have been roughly 1·16 times the true current entering the terminated segment. For the same fibre, the equivalent factor for the uncompensated total current would have been about 1·84.

RESULTS

Electrical resistance of fibre and gap

In the process of developing and testing the single gap system, electrical resistance measurements were made on twenty fibres ($0{\cdot}35 \leqslant l_c \leqslant 1{\cdot}12$ mm) with solution *C* in pool *C* and solution *A* in pool *A* (1–4 °C).

Using the steady changes in V_P, V_I and V_m accompanying 15–20 mV pulses applied to pool *A* from a 0 mV base line (see Methods), the effective resistance R_P between pools was calculated as $V_P R_I/V_I$. The mean ($\pm$ S.D.) value of R_P was $4{\cdot}3 \pm 3{\cdot}1$ MΩ, with individual values ranging from 1·6 to 15·5 MΩ. The fractional resistance $R_{IN}/(r_i l_B + R_{IN})$ contributed by the closed fibre segment to the resistance in the internal fibre path between pools was calculated as V_m/V_P. Its mean value was $0{\cdot}90 \pm 0{\cdot}09$, with a range of 0·71–1·00. Thus, the major portion of the resistance in the internal path was contributed by the closed fibre segment.

After having adjusted the compensating circuit, values of K_P and K_I were obtained from its settings and were used for further calculations. For the same fibres, the mean value of K_P was $0{\cdot}99 \pm 0{\cdot}09$, with individual values ranging from 0·81 to 1·22. With the compensating circuit properly set, however, K_P should equal $r_e/(r_i + r_e)$, which must be less than or equal to one. Compensating circuit settings with K_P values greater than one must thus have been in error. Excluding the five fibres having measured K_P values greater than one, $K_P = 0{\cdot}94 \pm 0{\cdot}05$ ($n = 15$).

A possible source of the error in K_P settings can be seen by referring to Fig. 5. Fig. 5*Aa* and *Ba* present superimposed V_m and V'_m oscilloscope traces from two different fibres for a 40 mV pulse applied to pool *A*. In 5*Aa*, the compensation was perfect and V'_m is superimposed on V_m. In 5*Ba*, however, the compensation was not perfect. In cases such as this, the compensating circuit was set so that the size of the transient component of $-V_I$ was scaled to equal the steady amplitude of V_m. V_P was then scaled so that the V'_m record showed no discontinuity at pulse ON and OFF. The resulting more rapid rise of V'_m than V_m indicates that V_I contained a fast transient component which did not totally contribute to the voltage drop across $r_i l_B$. This would be the case either if some current left the fibre before the point of electrode insertion or if V_I contained a component of current due to capacitative coupling between pools. The value of K_I would in such cases be set too high. As a result, the value of K_P which gave no jump in V'_m at pulse ON and OFF would also have to be set too high. Variation between compensation settings such as those in Fig. 5*Aa* and *Ba* may have been due to variations in the geometry of the Vaseline seal around the fibre.

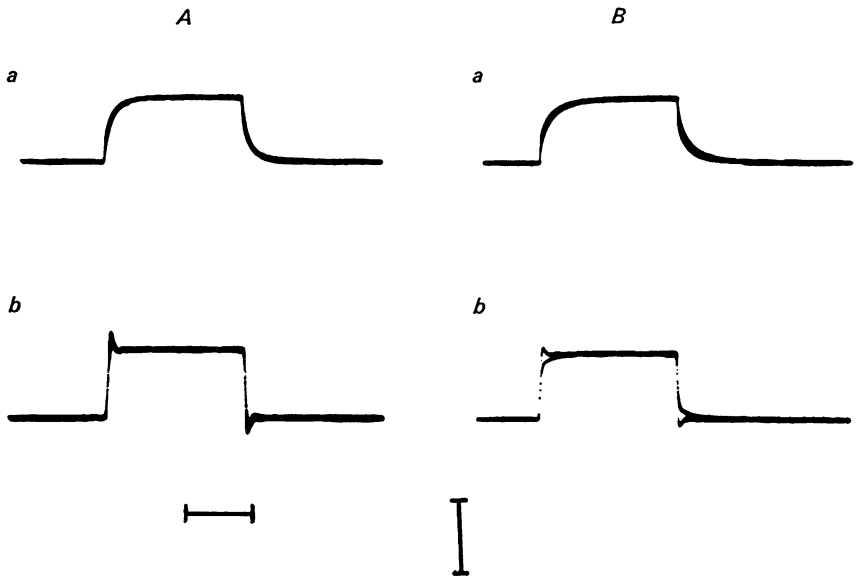

Fig. 5. Superimposed traces of V_m and V'_m from two different fibres, *A* and *B*. Records *a* are for a V_P pulse whereas records *b* are for voltage-clamp of V'_m. Horizontal calibration is 20 msec, vertical is 40 mV. Pools *A* and *C* contained solutions *A* and *C*. *A*, same fibre and conditions as in Fig. 4. *B*, fibre 72 with $l_c \simeq 550$ μm, $d = 90$ μm and $S = 2{\cdot}33$ μm (3·3 °C).

Using the K_P and K_I values for each fibre having a K_P value less than unity, the mean ($\pm$ S.D.) values of $r_i l_B$ and $r_e l_B$ were found to be $0{\cdot}45 \pm 0{\cdot}13$ MΩ and $15{\cdot}5 \pm 14{\cdot}4$ MΩ. The R_{IN} value for each of these fibres was calculated from its $r_i l_B$ and R_P values, giving a mean R_{IN} of $5{\cdot}9 \pm 4{\cdot}4$ MΩ.

The mean value of $R_P/r_e l_B$ of these fifteen fibres was $0{\cdot}36 \pm 0{\cdot}21$. Since $R_P/r_e l_B$ equals the ratio of external to total conductance between pools, it gives the fraction of steady current which passed between pools via the external resistance. Thus, on the average about one third of the steady current traversed the external leak and about two thirds traversed the fibre. This is illustrated by records *A* and *D* in Fig. 4 which show the steady current corresponding to V'_I to be about 0·65 times that of the steady current corresponding to V_I.

As a final check, l_B was calculated for each fibre by dividing $r_1 l_B$ by r_1. The r_1 values were determined using the internal resistivity of intact fibres (Hodgkin & Nakajima, 1972) and assuming circular fibre cross-sections of diameter d equal to the maximum fibre width measured in a plane perpendicular to the microscope axis. The eleven fibres in which d was measured and K_P was less than one gave $l_B = 677 \pm 259\ \mu m$, a value reasonably close to the 550 μm width of the wall separating the pools. This result is consistent with cut fibres having similar internal resistivities as intact fibres.

Voltage-clamping and fibre repolarization

After having set the compensating circuit, the voltage-clamp circuit was activated to control V_m'. Superimposed traces of V_m' and V_m for clamp pulses in two fibres are shown in the lower part of Fig. 5. For the fibre in which the compensation was exact for a V_P pulse (Fig. 5*Aa*), V_m also closely agreed with V_m' under voltage-clamp (Fig. 5*Ab*). This confirms the prediction that proper compensation should be independent of the V_P wave form. In the fibre in which V_m rose more slowly than V_m' for a V_P pulse (Fig. 5*Ba*), V_m also rose more slowly than V_m' under voltage-clamp (Fig. 5*Bb*). The V_m records for clamp pulses in the two situations indicate that the system as presently employed involves some uncertainty regarding V_m during the first few milliseconds of a clamp pulse.

After adjusting the compensating circuit and voltage clamping the fibre using a steady command voltage E_C of 0 mV, E_C was set at -104 to -107 mV. The exact E_C value was chosen so as to hold V_m' at -100 mV with the clamp gains of about 80 used in these experiments. Two types of fibre behaviour were subsequently observed during the first few minutes following repolarization. In about 80% of the cases V_P and V_I declined slightly during the first 3–5 min of repolarization. Except for subsequent small slow drifts of V_I with time, such fibres were electrically stable for periods of from one to up to 5–6 hr during which time depolarizing pulses to and beyond contraction threshold were applied. In the remaining approximately 20% of the fibres a large increase in V_P and V_I occurred within about 1–4 min of setting V_m' to -100 mV. This was followed by visible swelling and development of a contracture clot, sometimes in the closed segment but more often spreading out from the gap. Such fibres were discarded at this point. A puzzling aspect of this phenomena was that both groups of fibres had similar fibre and gap electrical properties when measured at membrane potentials close to 0 mV before repolarization.

Strength–duration relationship for contraction threshold

In order to reprime contractile activity completely at these relatively low temperatures (Hodgkin & Horowicz, 1960; Caputo, 1972), fibres were held at -100 mV for at least 10 min before continuing. Increasingly large depolarizing pulses were then applied to determine the contraction threshold. Pulses well above threshold caused large fibre movements at the tendon with relatively little fibre movement at the gap. For pulses at or just above the contraction threshold small movements were most often detected near the tendon, but in some cases threshold movements were observed at various other locations along the fibre.

Following repolarizations of more than 10 min contraction thresholds, routinely

monitored using 50–100 msec pulses, were found to be fairly stable with time. The strength–duration results reported here were obtained after at least 15–25 min at −100 mV.

Average strength–duration results from four fibres having TTX Ringer solution in pool *C* and solution *A* in pool *A* are presented in Fig. 6 (circles). For comparison, the contraction thresholds for 5, 10 and 100 msec pulses determined by Costantin (1974) using a two micro-electrode voltage clamp in intact fibres bathed in the same solution at the same temperature are also presented. The contraction thresholds of cut fibres are clearly very similar to those reported for intact fibres, indicating that the excitation–contraction coupling process must be relatively undisturbed in the cut fibres.

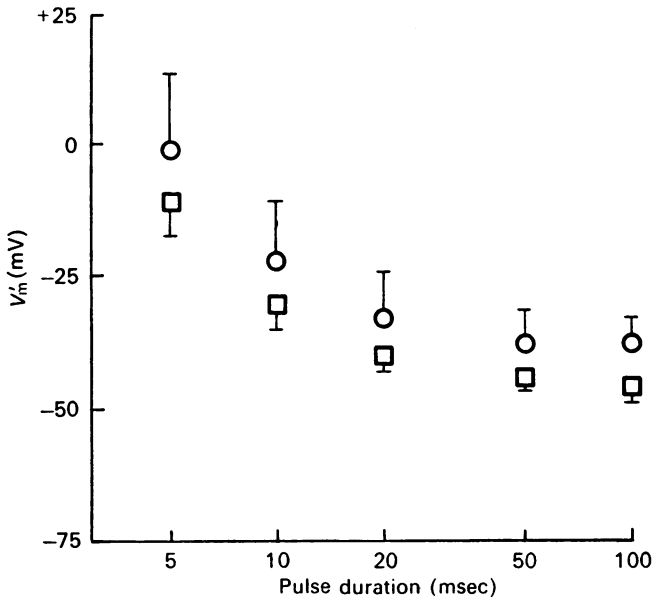

Fig. 6. Strength–duration curves for depolarizing pulses giving microscopically just detectable movement of cut and intact fibres. Circles: mean (± 1 S.D.) results from four cut fibres with TTX Ringer solution in pool *C* and solution *A* in pool *A* (3·4–4·3 °C). The l_c and *S* values in μm corresponding to each fibre (number in parentheses) were: 380, 3·01 (43); 406, 2·50 (44); 228, 2·38 (45); 355, 2·51 (46). Squares: results reported by Costantin (1974) for intact fibres using a two-micro-electrode voltage clamp. Weighted mean (± 1 S.D.) of results from thirteen fibres at 3·0 °C having mean S = 2·83 μm and eleven fibres at 3·9 °C having mean S = 3·30 μm.

Fig. 7 illustrates the effect on the strength–duration relationship of changing from Ringer solution to solution *C* in three of the fibres from Fig. 6. Solution *C*, which contained TEA and some rubidium as predominant cations and sulphate as predominant anion, was preferable to Ringer solution for voltage-clamp studies of contractile activation in gap clamped fibres since it decreased fibre conductances and thus tended to minimize steady-state potential decrement both along the fibre and into the T-system. Changing from Ringer solution to solution *C* caused a mean (± S.D.) negative shift of 7·9 ± 1·4 mV in the contraction threshold at all durations investigated. Similar shifts of −8·6 mV (Costantin, 1968) and −7·6 mV (Chandler,

Rakowski & Schneider, 1976*b*) in contraction thresholds of intact fibres for 200 msec pulses have been respectively observed when external sodium was replaced by TEA or when external sodium and potassium were replaced by TEA and rubidium, both in chloride-containing Ringer solutions. In the present case the TEA and rubidium solution had sulphate rather than chloride as anion so that its free calcium concentration was also presumably less than that of Ringer solution (cf. Hodgkin & Horowicz, 1959). In intact fibres in chloride-containing Ringer solution a 50% decrease in external calcium has been found to cause a shift of about −2·5 mV in contraction thresholds for 200 msec pulses (Costantin, 1968).

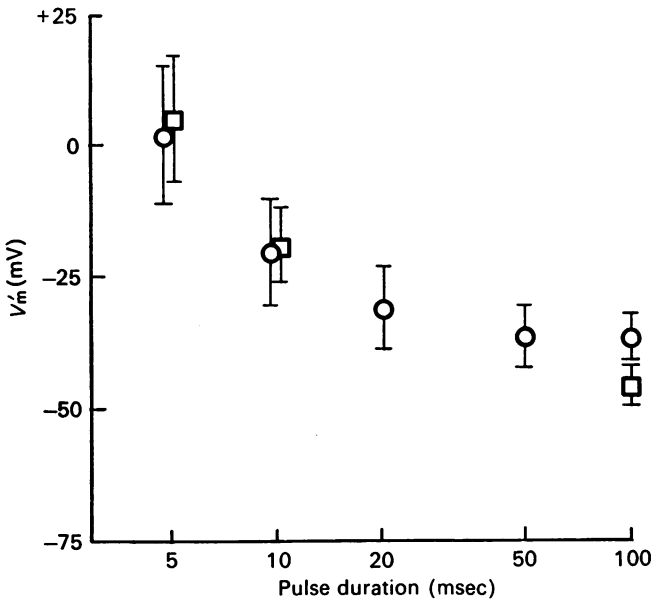

Fig. 7. Effect of TEA_2SO_4 solution on strength–duration curves for just detectable movement. Circles: TTX Ringer solution in pool *C* (3·6–3·7 °C). Squares: solution *C* in pool *C* (3·9–4·5 °C). Pool *A* contained solution *A* in both cases. Same fibres (numbers 43, 45 and 46 of Fig. 6 legend) studied in both external solutions. Error bars give 1 S.D.

In order to avoid the possibility of clamp oscillations due to compensation errors introduced in the process of changing external solutions, the voltage control circuit was disconnected during the solution change by putting the switch in Fig. 2 in position 2. Before disconnecting the clamp circuit E_p was first set equal to the output voltage of the clamp amplifier so that no depolarization or contraction occurred on unclamping. On completion of the solution change but before reconnecting the control circuit, the compensating circuit setting was checked and readjusted with the micro-electrode in the fibre. The voltage clamp circuit was then reactivated.

Most of the cut fibres which have thus far been studied were obtained either from winter frogs kept in a refrigerator at about 4 °C or from summer frogs refrigerated for at least a few days before use. Only one series of experiments was carried out using a shipment of summer frogs kept at room temperature. With either Ringer solution (Fig. 8) or solution *C* as external solution, the contraction thresholds at 3–4 °C of fibres from the room temperature adapted frogs tended to be higher at all pulse durations than those of fibres from cold adapted frogs. Since the cold and

room temperature adapted animals came from different shipments of frogs, it is possible that the difference in thresholds was due to a peculiarity of the frogs themselves rather than to their state of temperature adaptation. However, L. Kovács & G. Szücs (unpublished observation) have obtained similar results with cut fibres

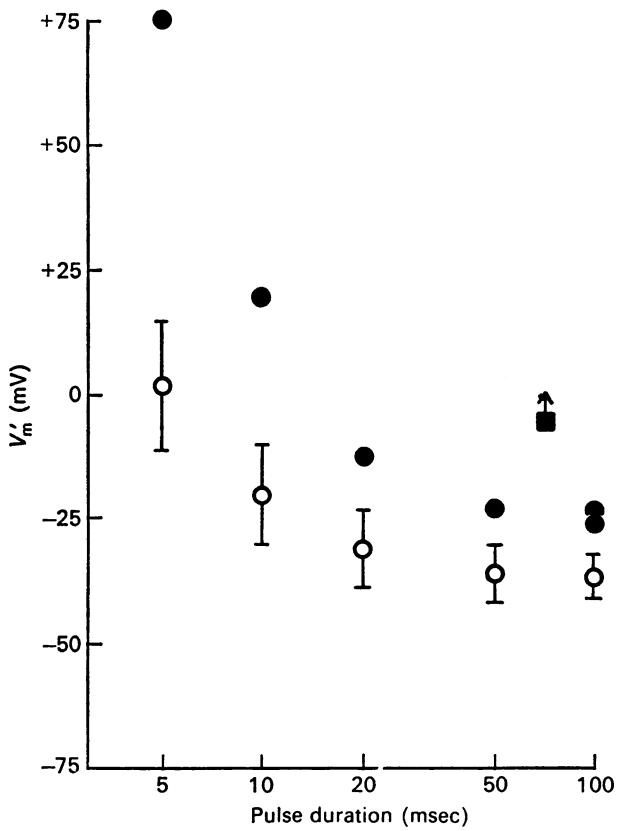

Fig. 8. Elevation of contraction threshold in fibres obtained from room temperature-adapted frogs. Open circles: mean (± 1 S.D.) strength–duration curve for just detectable movement of four fibres from cold-adapted frogs (same results as in Fig. 6). Filled circles: strength–duration curve for just detectable movement of a fibre from a room temperature adapted frog. Fibre 66 with l_c = 634 μm, d = 92 μm and S = 2·74 μm (3·8 °C). Filled square with arrow: indicates that a fibre from another room temperature-adapted frog exhibited no movement for a 70 msec depolarization to −5 mV. Fibre 64 with l_c = 500 μm, d = 84 μm and S = 2·69 μm (3·5 °C). Optical transparency changes recorded from this fibre appear in Fig. 3 of Kovács & Schneider, 1977*a*. TTX Ringer solution in pool *C* and solution *A* in pool *A* in all cases.

after adapting individual frogs from the same population to warm and cold temperatures. In addition, W. F. Gilly & C. S. Hui (personal communication) have observed that at 10 °C voltage-clamped intact fibres from cold-adapted frogs have lower thresholds for short pulses than do fibres from room temperature adapted frogs. Thus, the apparent temperature adaptation effect may be real.

Delayed rectification

Fig. 9 presents V_m' and V_I' records for a series of increasingly large depolarizing clamp pulses applied to a fibre with TTX Ringer solution in pool C and solution A in pool A. For negative (not illustrated) or small positive pulses the V_I' records exhibited a transient capacitative current which declined to a steady level. With larger depolarizations a delayed increase in outward current developed during the pulse. This outward delayed rectifier current became larger and developed faster with increasingly large depolarizations.

In order to separate the maximum delayed rectifier current at each V_m' from current through resting fibre conductances, the steady level of V_I' was plotted as a function of the steady level of V_m' during the pulse. For the largest depolarizations,

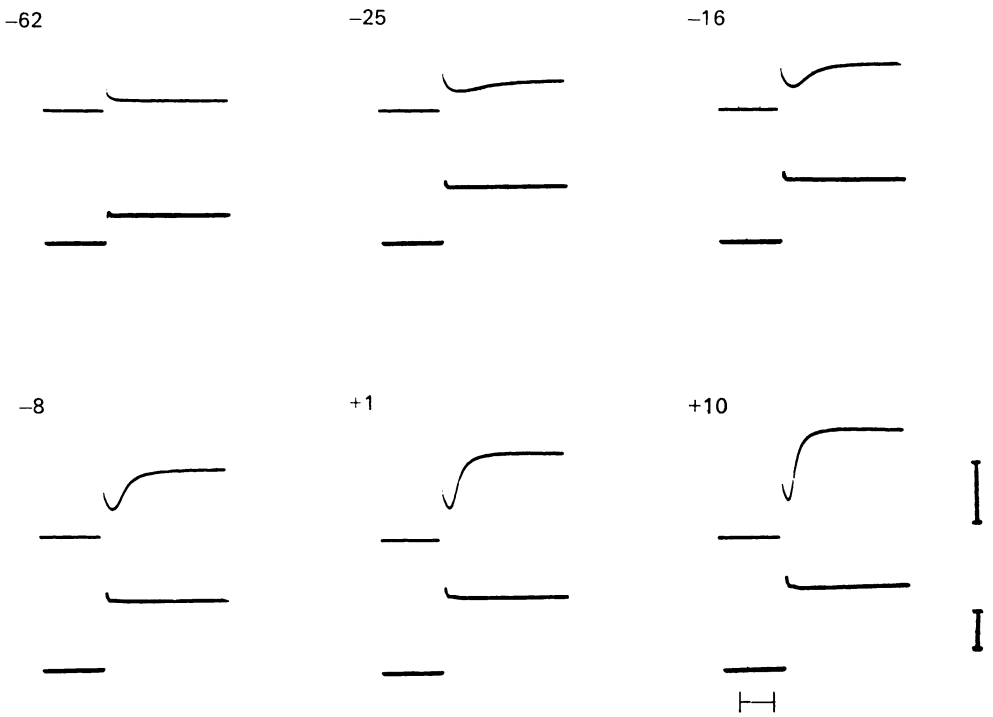

Fig. 9. Delayed rectifier currents observed during voltage-clamp depolarization of a cut muscle fibre. Photographs of oscilloscope records of V_I' (upper) and V_m' (lower) for pulses to the indicated V_m' levels (mV). V_m' and V_I' were obtained from two different oscilloscope beams which were slightly misaligned horizontally causing V_I' to appear to start slightly before V_m'. Most of the V_I' capacitative current transient was not captured in the photograph. Vertical calibrations are 20 μA/μF (V_I' converted to current normalized to total fibre capacitance) and 50 mV (V_m'). Horizontal calibration is 20 msec. Same fibre and conditions as represented by filled square in Fig. 8.

where the onset of delayed rectifier inactivation (Nakajima, Iwasaki & Obata, 1962; Adrian, Chandler & Hodgkin, 1970) sometimes caused a slight decline in V_I' during the pulse, the peak V_I' value was plotted. For negative and small positive pulses V_I' appeared to follow a linear relationship with V_m'. For the larger positive pulses

the difference between V_I' and the extrapolated linear component was taken as the current I_K through the delayed rectifier system.

The steady-state voltage dependence of delayed rectifier activation was analysed using the equation

$$I_K = n_\infty^4 \bar{g}_K l_c (V_m' - V_K), \tag{7}$$

where n_∞ is the fractional degree of delayed rectifier activation in the steady state at membrane potential V_m', $\bar{g}_K$ is the maximally activated delayed rectifier conductance per unit fibre length and V_K is the delayed rectifier reversal potential (Hodgkin & Huxley, 1952; Adrian *et al.* 1970). Arbitrarily assuming $V_K = -80$ mV, the I_K values for each V_m were divided by $V_m - V_K$ and the fourth root of the quotient determined. The result is proportional to n, with the proportionality factor being $(\bar{g}_K l_c)^{\frac{1}{4}}$.

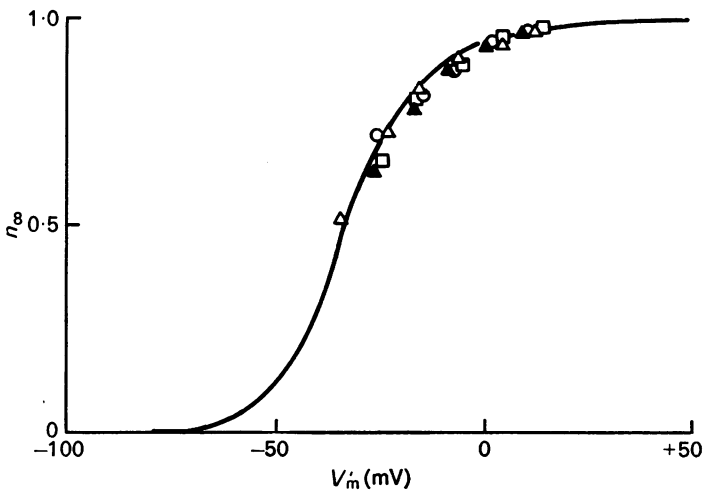

Fig. 10. Voltage-dependence of the steady-state value n_∞ of the Hodgkin–Huxley variable n for delayed rectification in cut muscle fibres. Open symbols give results from three fibres from cold-adapted frogs with TTX Ringer solution in pool *C* and solution *A* in pool *A* (3·7–3·9 °C). Same fibres, 43 (○), 45 (□) and 46 (△), as in Fig. 7. Filled triangles give results from a fibre from a room temperature-adapted frog. Same fibre and conditions as shown in Fig. 9 and also represented by filled square in Fig. 8. The values of n_∞ were calculated from records such as those in Fig. 9 as described in the text. The curve gives n_∞ as determined by Chandler *et al.* (1976*b*) in intact fibres in TTX Ringer solution made hypertonic by sucrose addition.

Since depolarizations large enough to bring n to 1 were not used, the proportionality factor for each fibre was set on the assumption that the relationship between n and V_m' would correspond to the theoretical curve of Adrian *et al.* (1970) shifted 12 mV in the positive direction as observed by Chandler *et al.* (1976*b*). A value of $(\bar{g}_K l_c)^{\frac{1}{4}}$ was selected for each fibre so as to make the value of n at a V_m' level close to 0 mV equal to the theoretical value of n at that voltage. The selected value of $(\bar{g}_K l_c)^{\frac{1}{4}}$ was then used to calculate n at all other V_m' levels. The resulting variation of n with V_m' determined in four fibres is presented in Fig. 10. At all voltages examined, the calculated n values lie close to the theoretical relationship, indicating a similar voltage dependence of delayed rectifier activation in intact and cut fibres.

The theoretical curve referred to in the preceding paragraph was determined in intact fibres bathed in sucrose hypertonic Ringer solution (Chandler *et al.* 1976*b*). In intact glycerol-treated fibres in isotonic Ringer solution the delayed rectifier n_∞ curve appeared to correspond to the theoretical curve of Adrian *et al.* (1970) shifted about 15–16 mV in the positive direction (W. K. Chandler, R. F. Rakowski & M. F. Schneider, unpublished observation). The theoretical curve in Fig. 10 must thus be shifted 3–4 mV in the positive direction in order to correspond to results for intact glycerol-treated fibres in isotonic solution. Such a curve would also agree with the present results obtained from cut fibres in isotonic solution.

An additional point concerning Fig. 10 is that the three fibres represented by open symbols are the same fibres from cold adapted frogs as used in Fig. 7. The fourth fibre, represented by the filled symbols in Fig. 10, is the same fibre from a room temperature adapted frog as represented by the square in Fig. 8. Thus, although adaptation to room temperature caused a large positive shift in the contraction threshold of the latter fibre, it caused little or no shift in its delayed rectifier activation curve. In addition, cold adaptation did not appear to alter the rate of activation of delayed rectification. Assuming n^4 kinetics (Adrian *et al.* 1970), delayed rectifier current will reach 66% of its steady level in 2·3 times the time constant τ_n for activation of n. Using this method of calculation, τ_n values in the three fibres from cold-adapted frogs were 3·0–4·5 msec at +12 to +14 mV and 5·6–10·0 msec at −15 mV. Corresponding values for the fibre from the warm adapted frog were 4·5 msec at +10 mV and 9·5 msec at −16 mV.

To compare amounts of delayed rectification in different-sized fibre segments, the maximum delayed rectifier conductance $\bar{g}_K l_c$ of each fibre was normalized to its total capacitance. Since the capacitance of the closed fibre segment is cl_c, where c is the fibre capacitance per unit length, normalization gives $\bar{g}_K/c$. Values of cl_c were determined for each fibre by integrating the capacitative current transients for small positive and negative pulses and dividing by the size of the corresponding V'_m step. The mean (± S.D.) value of $\bar{g}_K/c$ for the four fibres in Fig. 10 was 0·29 ± 0·17 mmho/μF. This is fairly close to the $\bar{g}_K/c$ values of 0·40 mmho/μF determined in intact fibres in hypertonic solution after correction for the elevated internal potassium concentration (Chandler *et al.* 1976*b*) and 0·39 mmho/μF determined in glycerol-treated intact fibres in isotonic solution after correcting for the decline in capacitance due to the glycerol treatment (Chandler *et al.* 1976*b*).

DISCUSSION

The main conclusion from the results presented here is that cut muscle fibres prepared according to the procedure employed in these studies provide a reasonable preparation for studying both excitation–contraction coupling and membrane conductances. The finding that 5–100 msec depolarizing pulses applied to electrically repolarized cut fibres produce threshold contractions at voltages close to those reported for intact fibres strongly indicates that the sequence of events leading from fibre depolarization to the initiation of threshold mechanical activity was undisturbed. Contractile activation for controlled pulses well above contraction threshold could also be studied in cut fibres without damage. Isometric contractions giving relatively large amounts of tension development do not, however, appear to be feasible with gap clamped fibres since the activated segment would tend to shorten

while extending the non-activated segment in the gap (Nakajima & Bastian, 1974). The findings that cut and intact fibres exhibit similar shifts in contraction threshold strength–duration curves in TEA-containing solutions and similar amounts and steady-state activation curves of delayed rectification all tend to support the general conclusion that membrane properties of cut and intact fibres are similar.

A major advantage of cut over intact fibres is that in the former the internal solution composition can be altered according to the solution applied to the cut end. Using the optical apparatus previously described (Kovács & Schneider, 1977*a*) to measure absorption spectra of fibre segments in pool *C*, it has repeatedly been observed that a 284 molecular weight dye added at 0·5–1 mM concentration to pool *A* entered the terminated fibre segment and attained a constant level in less than about 1·5 hr (unpublished observation). It has also been found that the small delayed outward currents observed with relatively large depolarizations even in high external TEA concentrations in both intact (Stanfield, 1970; Chandler *et al.* 1976*a*) and cut fibres are not observed when caesium glutamate is used in place of potassium glutamate in solution *A* in pool *A* (P. Horowicz & M. F. Schneider, unpublished observation), indicating entry of caesium into the terminated segment.

In view of the above evidence for equilibration between the pool *A* solution and fibre interior in pool *C*, it is somewhat surprising that several hours incubation with 1 mM-EGTA in pool *A* did not appear to raise contraction thresholds. One possible explanation is that due to interaction with various components inside the fibre, the effective diffusion coefficient of EGTA in the myoplasm was very much reduced so that little reached the segment in pool *C*. An alternative explanation is that the EGTA did equilibrate with the terminated segment but that its calcium-binding kinetics are slow (Smith, Berger, Podolsky & Czerlinski, 1977) compared with those of troponin and of the sarcoplasmic reticulum so that little of the released calcium was complexed EGTA.

The finding that room temperature adaptation appears to elevate contraction thresholds at low temperatures may prove to be convenient for studies of early steps in excitation contraction coupling using techniques which require elimination of fibre movement. For example, fibre transparency changes without movement artifacts have been recorded from cut fibres of room temperature adapted frogs using pulses which would have produced movement of fibres from cold adapted frogs (Kovács & Schneider, 1977*a*). Previous findings related to the effect of adaptation temperature on skeletal muscle contraction include a marked decrease of contractile ability at temperatures below 9 °C in intact single fibres from tropical frogs (Caputo, 1976) and depression of both tetanic tension (Hajdu, 1951) and of metabolic activity (Rieck, Belli & Blaskovics, 1960) at low temperatures in whole frog muscles from warm-adapted frogs. The latter observation, together with the present finding that at low temperature fibres from room temperature-adapted frogs may lack movement but have normal delayed rectification, is consistent with adaptation temperature's affecting the late mechanochemical steps in excitation–contraction coupling while perhaps not affecting the earlier membrane-related processes.

APPENDIX

Analysis of voltage and current recorded using the single gap with compensating circuit

The equations presented in the Theory section were derived on the basis of the approximate fibre and gap circuit shown in Fig. 3*A*. Since that circuit is strictly valid only for the case of negligible membrane conductance within the gap, the equations may be in error if significant membrane current flows within the gap. In this appendix we apply a complete cable analysis to the gap segment making no assumption regarding its membrane conductance. The results show (i) that the compensating circuit method for voltage recording is valid independent of the gap membrane conductance, and (ii) that the current recorded using the compensating circuit is larger than the true internal current entering the terminated segment. The magnitude of the current over-estimate is evaluated in terms of a multiplicative correction factor. In all cases, the compensated current is less of an over-estimate than would have been obtained using the uncompensated total current.

Voltage recording

Starting from the cut end side of the gap, the internal potential V_i and external potential V_e are given as functions of the distance y into the gap by

$$V_i = V_P - r_i \int_0^y I_i \, dy \tag{1A}$$

and

$$V_e = V_P - r_e \int_0^y I_e \, dy. \tag{2A}$$

r_i and r_e are assumed to be constant across the gap. Although I_i and I_e may vary with y, the total current I is independent of y. Using this fact and the relationship $I = I_i + I_e$, eqn. (1A) gives

$$V_i = V_P + r_i \int_0^y I_e \, dy - r_i I \int_0^y dy. \tag{3A}$$

The first integral in eqn. (3A) can be determined by rearranging eqn. (2A) and the second integral can be directly evaluated, thus giving

$$V_i = V_P(r_i + r_e)/r_e - V_e(r_i/r_e) - r_i I y. \tag{4A}$$

At the point $y = l_B$, which corresponds to the beginning of the terminated segment beyond the gap, $V_e = 0$ and V_i equals the input voltage V_m of the terminated segment. Consequently, eqn. (4A) at $y = l_B$ is identical to eqn. (3) in the Theory section. Use of the compensation procedure for voltage recording and for determining the internal and external gap resistances is thus valid, independent of the membrane resistance in the gap. A similar conclusion regarding gap r_i and r_e measurements was obtained by New & Trautwein (1972) for slightly different boundary conditions. However, these authors failed to recognize that the validity of assuming infinite gap membrane resistance for r_i and r_e determinations does not establish the validity of the same assumption for separating internal and external current components.

It should be noted that the preceding analysis is general in that it applies to both steady-state and transient conditions. The compensating circuit method of voltage recording is thus valid for both steady and changing voltages.

Current measurement

The general equation for the steady-state membrane potential V within the gap as a function of distance y across the gap is

$$V = A \sinh y/\lambda_B + B \cosh y/\lambda_B. \tag{5A}$$

A and B are constants and λ_B is equal to $[r_m/(r_i+r_e)]^{\frac{1}{2}}$, where r_m denotes the fibre membrane resistance within the gap.

The first boundary condition on eqn. (5A) is that V at the cut end, $y = 0$, is zero. This gives $B = 0$.

The second boundary condition is that the internal current leaving the gap must equal the current entering the terminated segment. The latter is given by the ratio of the terminated segment's input voltage V_m to its input resistance R_{IN}. The equation for I_i is

$$I_i = \frac{-1}{r_i}\frac{dV_i}{dy}. \tag{6A}$$

dV_i/dy can be obtained by substituting $V_i - V$ for V_e in eqn. (4A), solving for V_i and differentiating. Substituting the result in eqn. (6A) gives

$$I_i = \frac{-1}{r_i+r_e}\frac{dV}{dy} + \frac{Ir_e}{r_i+r_e}. \tag{7A}$$

Eqn. (7A) can now be evaluated to determine I_i at $y = l_B$. dV/dy at $y = l_B$, obtained from eqn. (5A), is $(A/\lambda_B)\cosh l_B/\lambda_B$. I is obtained from eqn. (3) using $A \sinh l_B/\lambda_B$ for V_m. Equating the resulting expression for I_i at $y = l_B$ to the expression for V_m/R_{IN} gives

$$\frac{A \sinh l_B/\lambda_B}{R_{IN}} = -\frac{A \cosh l_B/\lambda_B}{(r_i+r_e)\lambda_B} + \frac{V_P}{r_i l_B} - \frac{r_e A \sinh l_B/\lambda_B}{(r_i+r_e)\, r_i l_B}. \tag{8A}$$

Solving eqn. (8A) for A gives

$$A = \frac{V_P}{r_i l_B}\left[\left(\frac{1}{R_{IN}} + \frac{r_e}{(r_i+r_e)\, r_i l_B}\right)\sinh l_B/\lambda_B + \frac{\cosh l_B/\lambda_B}{(r_i+r_e)\,\lambda_B}\right]^{-1}. \tag{9A}$$

The input voltage $A \sinh l_B/\lambda_B$ of the terminated segment is thus

$$V_m = V_P[r_i l_B(R_{IN}+R_B)/R_{IN}R_B + r_e/(r_i+r_e)]^{-1}, \tag{10A}$$

where resistance R_B is defined by

$$R_B = (r_i+r_e)\,\lambda_B \tanh l_B/\lambda_B. \tag{11A}$$

R_B corresponds to the input resistance of a length l_B of gap fibre terminated by zero resistance. The current V_m/R_{IN} entering the terminated segment is obtained directly from eqn. (10A) by dividing by R_{IN}.

Assuming zero gap membrane conductance, the current $I_i(l_B)$ entering the terminated segment at $y = l_B$ was approximated as

$$I_i(l_B) \approx (V_P - V_m)/r_i l_B. \tag{12A}$$

To make this expression exact, a multiplicative correction factor k can be introduced so that

$$I_i(l_B) = k(V_P - V_m)/r_i l_B, \tag{13A}$$

where k is defined by

$$k = r_i l_B V_m / R_{IN}(V_P - V_m). \tag{14A}$$

Substituting the expression in eqn. (10A) for V_m and rearranging,

$$k = \left[1 + R_{IN}\left(\frac{1}{R_B} - \frac{1}{(r_i + r_e)\, l_B}\right)\right]^{-1}. \tag{15A}$$

For small values of l_B/λ_B, R_B approaches $(r_i + r_e)\, l_B$ and k approaches 1. This corresponds to the approximate circuit having negligible gap membrane conductance. For larger values of l_B/λ_B, R_B is less than $(r_i + r_e)\, l_B$ so that k is less than unity. The smaller the value of R_{IN}, the closer k will be to 1. In practice, however, the degree to which R_{IN} can be reduced by using terminated segments which are longer or have higher membrane conductances is limited by the amount of tolerable voltage non-uniformity along the terminated segment. This limitation has not been dealt with in this analysis, but has been considered by McGuidan & Tsien (1974) in a more general analysis of errors in membrane current recording using single or double gap arrangements.

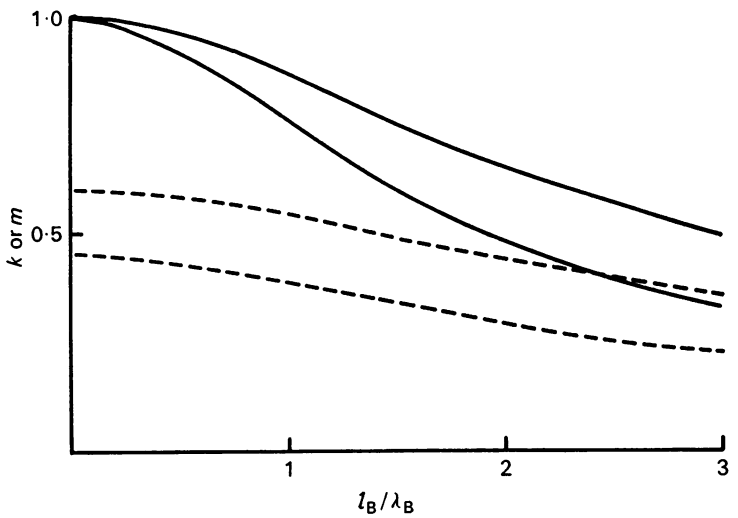

Fig. 11. Multiplicative factors for correcting currents from fibres in a single gap chamber. The continuous curves give the factor k used to correct the current recorded with a properly adjusted compensating circuit. k was calculated according to eqn. (16A) with $R_{IN}/(r_i + r_e)\, l_B$ equal to 0·5 for the upper k curve and 1·0 for the lower one. The interrupted curves give the factor m used to correct the uncompensated total current. m was calculated according to eqn. (18A) with $R_{IN}/(r_i + r_e)\, l_B$ equal to 0·5 for the upper m curve and 1·0 for the lower one so that the upper and lower m curves should be compared with the respective k curves. $r_e/(r_i + r_e)$ was equal to 0·9 for calculating both m curves.

Substituting eqn. (11A) into (15A) and rearranging gives

$$k = \{1 + [R_{IN}/(r_i + r_e)\, l_B]\, [(l_B/\lambda_B) \coth l_B/\lambda_B - 1]\}^{-1}. \tag{16A}$$

Graphs of k as a function of l_B/λ_B for two values of $R_{IN}/(r_i + r_e)\, l_B$, 0·5 and 1·0, are given respectively by the upper and lower continuous curves in Fig. 11. r_m is the only variable in l_B/λ_B that does not also appear in $R_{IN}/(r_i + r_e) l_B$. It is thus

the only one that can be independently varied to alter l_B/λ_B while remaining on a given k curve of the type shown in Fig. 11. When l_B/λ_B is altered by varying r_i, r_e or l_B, it is also necessary to adjust R_{IN} appropriately in order to remain on the given curve. A change in r_i, r_e or l_B with R_{IN} constant specifies not only a new value of l_B/λ_B but also a new curve corresponding to the altered value of $R_{IN}/(r_i+r_e)\,l_B$.

The value of λ_B in these experiments could not be determined. However, a rough approximation can be made on the basis of other data. The space constant of intact 150 μm diameter semitendinosus fibres bathed in Ringer solution at 2–4 °C is about 3·0 mm (Hodgkin & Nakajima, 1972), which would correspond to $3{\cdot}0\,(60/150)^{\frac{1}{2}}$ or 1·9 mm for fibres of 60 μm diameter. Isotonic replacement of the chloride in Ringer solution by an impermeant anion causes about a threefold decrease in membrane conductance (Hodgkin & Horowicz, 1959; Hutter & Noble, 1960). In chloride-free solutions, increasing external potassium from 2·5 to 100 mM causes membrane conductance to increase by a factor of about 3 (Adrian & Freygang, 1962). Thus, fibre membrane conductances and space constants should be approximately the same in solution A as in Ringer solution. To account for the effect of r_e, the λ value of a fibre in free solution must be multiplied by $[r_i/(r_i+r_e)]^{\frac{1}{2}}$. Since $r_i/(r_i+r_e)$ was about 0·1, λ_B should have been about 0·6 mm and l_B/λ_B about 1. Using this value and the value consistent with experimental results of 0·5 for $R_{IN}/(r_i+r_e)\,l_B$, k is 0·86.

For a particular fibre in given solutions r_m, r_i and R_{IN} are set, whereas r_e and l_B may be adjusted by altering the gap geometry. It is thus of interest to examine the effects of separately altering either r_e or l_B. Increasing r_e or decreasing l_B both bring k closer to unity. For example, starting from the point $k = 0{\cdot}86$ at $l_B/\lambda_B = 1$ on the upper continuous curve in Fig. 11, quadrupling (r_i+r_e) causes k to go to 0·88 at $l_B/\lambda_B = 2$ on a higher curve, not presented in Fig. 11, for $R_{IN}/(r_i+r_e)\,l_B = 0{\cdot}125$, whereas halving l_B causes k to go to 0·92 at $l_B/\lambda_B = 0{\cdot}5$ on the lower curve for $R_{IN}/(r_i+r_e)\,l_B = 1{\cdot}0$. As l_B approaches zero, k approaches unity. This is true despite the increase in external leakage current with decreasing gap width because the compensating circuit makes a correction for external leakage current. In contrast, the uncorrected total current becomes an increasingly poor measure of $I_i(l_B)$ as l_B is decreased.

The error which would have been introduced by using the total current to approximate $I_i(l_B)$ can be determined from the relationship between $I_i(l_B)$ and I in eqn. (7A). At $y = l_B$, $(dV/dy)/(r_i+r_e)$ is equal to V_m/R_B, which in turn equals

$$I_i(l_B)\,R_{IN}/R_B.$$

Substituting this into eqn. (7A) and rearranging gives

$$I_i(l_B) = mI, \tag{17A}$$

where m is defined as

$$m = [R_B/(R_B+R_{IN})]\,[r_e/(r_i+r_e)]. \tag{18A}$$

m is thus the multiplicative factor which corrects the over-estimate of $I_i(l_B)$ that would have been obtained using I. Comparison of m and k shows that for any set of parameters, $1 \geqslant k \geqslant m \geqslant 0$. The compensated current thus approximates $I_i(l_B)$

more closely than I does. This is illustrated graphically in Fig. 11, where the dashed curves give m as a function of l_B/λ_B for the same values of $R_{IN}/(r_i+r_e)\,l_B$ as were used to calculate the continuous k curves. To calculate the m curves in Fig. 11 the parameter $r_e/(r_i+r_e)$, which does not enter the k calculation, was set equal to 0·9, a value consistent with the experimental results.

We are grateful to Dr P. Horowicz for participating in some of the experiments in which fibre and gap resistances were determined. This work was partially supported by grants from the U.S. National Institutes of Health (Research Career Development Award 5-K04-NS00078 to M.F.S. and Program Project NSPA-5-P01-NS20981) and the Muscular Dystrophy Association. L.K. was supported by a Muscular Dystrophy Association Fellowship.

REFERENCES

ADRIAN, R. H., CHANDLER, W. K. & HODGKIN, A. L. (1970). Voltage clamp experiments in striated muscle fibres. *J. Physiol.* **208**, 607–644.

ADRIAN, R. H. & FREYGANG, W. H. (1962). The potassium and chloride conductance of frog muscle membrane. *J. Physiol.* **163**, 61–103.

CAPUTO, C. (1972). The effect of low temperature on the excitation–contraction coupling phenomena of frog single muscle fibres. *J. Physiol.* **223**, 461–482.

CAPUTO, C. (1976). The effect of caffeine and tetracaine on the time course of potassium contractures of single muscle fibres. *J. Physiol.* **255**, 191–207.

CHANDLER, W. K., RAKOWSKI, R. F. & SCHNEIDER, M. F. (1976*a*). A non-linear voltage dependent charge movement in frog skeletal muscle. *J. Physiol.* **254**, 245–283.

CHANDLER, W. K., RAKOWSKI, R. F. & SCHNEIDER, M. F. (1976*b*). Effects of glycerol treatment and maintained depolarization on charge movement in skeletal muscle. *J. Physiol.* **254**, 285–316.

COSTANTIN, L. L. (1968). The effect of calcium on contraction and conductance thresholds in frog skeletal muscle. *J. Physiol.* **195**, 119–132.

COSTANTIN, L. L. (1974). Contractile activation in frog skeletal muscle. *J. gen. Physiol.* **63**, 657–674.

COSTANTIN, L. L. & PODOLSKY, R. J. (1967). Depolarization of the internal membrane system in the activation of frog skeletal muscle. *J. gen. Physiol.* **50**, 1101–1124.

EBASHI, S. & ENDO, M. (1968). Ca ion and muscle contraction. *Prog. Biophys. molec. Biol.* **18**, 123–183.

EBASHI, S., ENDO, M. & OHTSUKI, I. (1969). Control of muscle contraction. *Q. Rev. Biophys.* **2**, 351–384.

ENDO, M., TANAKA, M. & OGAWA, Y. (1970). Calcium induced release of calcium from the sarcoplasmic reticulum of skinned skeletal muscle fibres. *Nature, Lond.* **228**, 34–36.

FORD, L. E. & PODOLSKY, R. J. (1972). Calcium uptake and force development by skinned muscle fibres in EGTA buffered solutions. *J. Physiol.* **223**, 1–19.

HAJDU, S. (1951). Observations on the temperature dependence of the tension developed by the frog muscle. *Archs. int. Physiol.* **59**, 58–61.

HILLE, B. & CAMPBELL, D. T. (1976). An improved Vaseline gap voltage clamp for skeletal muscle fibres. *J. gen. Physiol.* **67**, 265–293.

HODGKIN, A. L. & HOROWICZ, P. (1959). The influence of potassium and chloride ions on the membrane potential of single muscle fibres. *J. Physiol.* **148**, 127–160.

HODGKIN, A. L. & HOROWICZ, P. (1960). Potassium contractures in single muscle fibres. *J. Physiol.* **153**, 386–403.

HODGKIN, A. L. & HUXLEY, A. F. (1952). A quantitative description of membrane current and its application to conduction and excitation in nerve. *J. Physiol.* **117**, 500–544.

HODGKIN, A. L., HUXLEY, A. F. & KATZ, B. (1952). Measurement of current–voltage relations in the membrane of the giant axon of *Loligo*. *J. Physiol.* **116**, 424–448.

HODGKIN, A. L. & NAKAJIMA, S. (1972). The effect of diameter on the electrical constants of frog skeletal muscle fibres. *J. Physiol.* **221**, 105–120.

HUTTER, O. F. & NOBLE, D. (1960). The chloride conductance of frog skeletal muscle. *J. Physiol.* **151**, 89–102.

HUXLEY, A. F. & STRAUB, R. W. (1958). Local activation and interfibrillar structures in striated muscle. *J. Physiol.* **143**, 40–41*P*.

HUXLEY, A. F. & TAYLOR, R. E. (1958). Local activation of striated muscle fibres. *J. Physiol.* **144**, 426–551.

JÖBSIS, F. F. & O'CONNOR, M. J. (1966). Calcium release and reabsorption in the sartorius muscle of the toad. *Biochem. biophys. Res. Commun.* **25**, 246–252.

KOVÁCS, L. & SCHNEIDER, M. F. (1977*a*). Increased optical transparency associated with excitation–contraction coupling in voltage-clamped cut muscle fibres. *Nature, Lond.* **265**, 556–560.

KOVÁCS, L. & SCHNEIDER, M. F. (1977*b*). Contractile activation by voltage clamp depolarization of cut muscle fibres. *Biophys. J.* **17**, 5*a*.

KUFFLER, S. W. (1946). The relation of electric potential changes to contracture in skeletal muscle. *J. Neurophysiol.* **9**, 367–377.

MCGUIGAN, J. A. S. & TSIEN, R. W. (1974). Appendix of MCGUIGAN, J. A. S. Some limitations of the double sucrose gap and its use in a study of the slow outward current in mammalian ventricular muscle. *J. Physiol.* **240**, 775–806.

NAKAJIMA, S. & BASTIAN, J. (1974). Double sucrose gap method applied to single muscle fiber of *Xenopus laevis*. *J. gen. Physiol.* **63**, 235–256.

NAKAJIMA, S., IWASAKI, S. & OBATA, K. (1962). Delayed rectification and anomalous rectification in frog's skeletal muscle membrane. *J. gen. Physiol.* **46**, 97–115.

NAKAJIMA, Y. & ENDO, M. (1973). Release of calcium induced by 'depolarization' of the sarcoplasmic reticulum membrane. *Nature, New Biol.* **246**, 216–218.

NATORI, R. (1954). The property and contraction process of isolated myofibrils. *Jikeikai Med. J.* **1**, 119–126.

NEW, W. & TRAUTWEIN, W. (1972). Inward membrane currents in mammalian myocardium. *Pflügers Arch.* **334**, 1–23.

RIECK, A. F., BELLI, J. A. & BLASKOVICS, M. E. (1960). Oxygen consumption of whole animal and tissues in temperature acclimated amphibians. *Proc. Soc. exp. Biol. Med.* **103**, 436–439.

SCHNEIDER, M. F. & CHANDLER, W. K. (1976). Effects of membrane potential on the capacitance of skeletal muscle fibers. *J. gen. Physiol.* **67**, 125–163.

SMITH, P. D., BERGER, R. L., PODOLSKY, R. J. & CZERLINSKI, G. (1977). Stopped-flow study of the rate of calcium binding by EGTA. *Biophys. J.* **17**, 159*a*.

STANFIELD, P. R. (1970). The effect of tetraethylammonium ion on the delayed currents of frog skeletal muscle. *J. Physiol.* **209**, 209–229.

STEN-KNUDSEN, O. (1954). The ineffectiveness of the 'window field' in the initiation of muscle contraction. *J. Physiol.* **125**, 396–404.

STEN-KNUDSEN, O. (1960). Is muscle contraction initiated by internal current flow? *J. Physiol.* **151**, 363–384.

TAYLOR, S. R., RÜDEL, R. & BLINKS, J. R. (1975). Calcium transients in amphibian muscle. *Fedn Proc.* **34**, 1379–1381.